Spectroscopic and Electrochemical Studies on Structural Change of Plastocyanin and Its Tyrosine 83 Mutants Induced by Interaction with Lysine Peptides†

Shun Hirota,*,‡ Kozue Hayamizu,‡ Takashi Okuno,‡ Mamiko Kishi,‡ Hideo Iwasaki,§ Takao Kondo,§ Takashi Hibino,|| Teruhiro Takabe,⊥ Takamitsu Kohzuma,# and Osamu Yamauchi‡,▽

Department of Chemistry and Division of Biological Science, Graduate School of Science, and Research Center for Materials Science, Nagoya University, Chikusa-ku, Nagoya 464-8602, Japan, Department of Chemistry, Faculty of Science & Technology, and Research Institute, Meijo University, Tempaku-ku, Nagoya 468-8502, Japan, and Department of Chemistry, Faculty of Science, Ibaraki University, Mito, Ibaraki 310-8512, Japan

Received December 29, 1999; Revised Manuscript Received March 14, 2000

ABSTRACT: Interactions of wild-type and Tyr83 mutant (Y83F, Y83S, Y83L, and Y83H) plastocyanins (PCs) with lysine peptides as models for the PC interacting site of cytochrome *f* have been studied by absorption, resonance Raman, and electron paramagnetic resonance (EPR) spectroscopies and electrochemical measurements. The spectral and electrochemical properties of PCs corresponded well with each other; species having a longer wavelength maximum for the S(Cys) $\pi \rightarrow$ Cu $3d_{x^2-y^2}$ charge transfer (CT) band observed around 600 nm and a stronger intensity for the 460-nm absorption band exhibited stronger intensities for the positive Met $\rightarrow$ Cu $3d_{x^2-y^2}$ and negative His $\pi_1 \rightarrow$ Cu $3d_{x^2-y^2}$ circular dichroism (CD) bands at about 420 and 470 nm, respectively, a lower average ν_{Cu-S} frequency, a smaller $|A_{||}|$ EPR parameter, and a higher redox potential, properties all related to a weaker Cu−S(Cys) bond and a more tetrahedral planar geometry for the Cu site. Similarly, on oligolysine binding to wild-type and several Tyr83 mutant PCs, a longer absorption maximum for the 600-nm CT band, a stronger intensity for the 460-nm absorption band, stronger 420-nm positive and 470-nm negative CD bands, and a lower average ν_{Cu-S} frequency were observed, suggesting that PC assumes a slight more tetrahedral geometry on binding of oligolysine. Since changes were observed for both wild-type and Tyr83 mutant PCs, the structural change due to binding of oligolysine to PC may not be transmitted through the path of Tyr83−Cys84−copper by a cation−π interaction which is proposed for electron transfer.

The structure−function relationship is one of the major topics in protein research. Type 1 copper proteins are classified from their unique spectroscopic properties as those exhibiting a low-energy ligand-to-metal charge transfer (LMCT)[1] band near 600 nm in their absorption spectra and a narrow hyperfine coupling constant ($|A_{||}| < 90 \times 10^{-4}$ cm^{-1}) in their electron paramagnetic resonance (EPR) spectra (*1*, *2*). Detailed studies on the relationship between the structure and the spectroscopic properties of type 1 copper proteins have been reported (*2*−*12*). Lu et al. mentioned that the ratio of the intensity of the 460-nm absorption band to that of the 600-nm band correlates with the rhombicity of the EPR signal for type 1 copper proteins (*5*). This rhombic distortion has been suggested to be associated with a stronger binding of the axial ligand and a concomitant shift from a trigonal planar toward a more tetrahedral Cu site geometry (*5*−*7*). It has been also shown that the Cu−S(Cys) stretching (ν_{Cu-S}) frequency is closely related to the electron-transfer exothermicity for several type 1 copper proteins (*8*). Dave et al. and Andrew et al. reported that the ν_{Cu-S} frequency is a sensitive probe of the Cu−S(Cys) bond strength and copper coordination geometry for proteins with cysteine thiolate coordination (*9*−*12*).

Plastocyanin (PC), a mobile type 1 copper protein existing in the thylakoid lumen of photosynthetic organisms, accepts an electron from cytochrome *f* (cyt *f*), a subunit of the cytochrome b_6f complex, and donates it to the reaction center chlorophyll ($P700^+$) in the photosystem I (PSI) complex (*13*−*15*). According to the crystal structures of oxidized and reduced plant PCs (*16*−*19*), PC contains one copper atom with two histidine nitrogen atoms, one methionine sulfur atom, and one cysteine sulfur atom coordinated in a distorted tetrahedral geometry. Plant PC usually possesses two highly conserved sites which have been considered as molecular recognition sites for its redox partners, cyt *f* and PSI: One site is located at the Cu-coordinated, solvent-accessible histidine (Cu-adjacent hydrophobic patch), and the other site

† This work was supported by Grants-in-Aid for Scientific Research to O.Y. and S.H. (09304062) and for Encouragement of Young Scientists to S.H. (10740304) from the Ministry of Education, Science, Sports, and Culture of Japan, and by a Grant-in-Aid from the Ground Experiment for the Space Utilization from the Japan Space Forum and National Space Developments Agency of Japan to T. Kohzuma.

* To whom correspondence should be addressed at the Department of Chemistry, Graduate School of Science, Nagoya University, Chikusa-ku, Nagoya 464-8602, Japan (Phone: +81-52-789-2952; Fax: +81-52-789-2953; e-mail: k46230a@nucc.cc.nagoya-u.ac.jp).

‡ Department of Chemistry, Nagoya University.

§ Division of Biological Science, Nagoya University.

|| Department of Chemistry, Meijo University.

⊥ Research Institute, Meijo University.

Ibaraki University.

▽ Research Center for Materials Science, Nagoya University.

[1] Abbreviations: PC, plastocyanin; cyt *f*, cytochrome *f*; cyt *c*, cytochrome *c*; PSI, photosystem I; CD, circular dichroism; RR, resonance Raman; EPR, electron paramagnetic resonance; CT, charge transfer; LMCT, ligand-to-metal charge transfer; ν_{Cu-S}, Cu−S(Cys) stretching.

10.1021/bi9929812 CCC: $19.00
Published on Web 05/05/2000

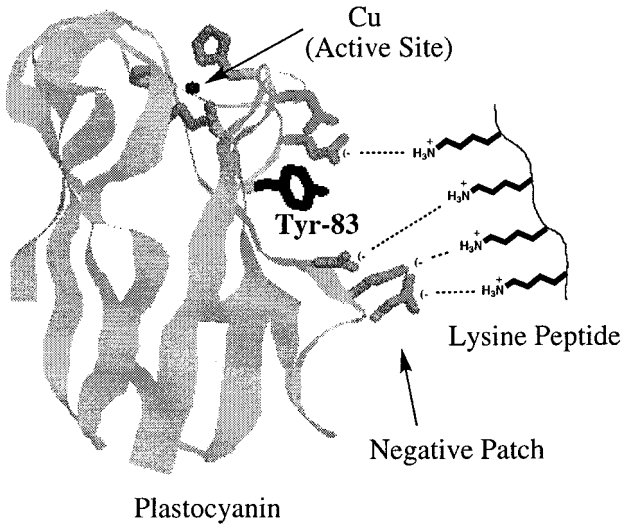

FIGURE 1: Schematic view of poplar PC interacting with *tetra*-Lys. Note that silene and spinach PC have four consecutive acidic residues at the lower site of its negative patch.

is located at another solvent-accessible site containing acidic residues near Tyr83 (Cu-remote negative patch) (Figure 1). However, experimental studies (*20*−*27*) and computational analyses based on electrostatic forces (*28*, *29*) have indicated that the Cu-remote negative patch is the cyt *f* molecular recognition site through electrostatic interactions.

The association constants between PC and cyt *f* or cytochrome *c* (cyt *c*) have been obtained by measuring the increase of the Soret band intensity of cyt *f* or cyt *c* on PC binding (*30*−*32*). An NMR study on the Cd-substituted PC−cyt *c* complex indicated that the PC−cyt *c* complex consists of a highly dynamic ensemble of structures (*33*), whereas a dynamic analysis of the electrostatics of PC and cyt *f* demonstrated three docked complexes (*34*). However, a recent paramagnetic NMR and restrained rigid-body molecular mechanics study indicated that the electrostatic interactions guide PC and cyt *f* into a position that is optimal for electron transfer (*35*). Kostić et al. proposed that PC and cyt *f* or cyt *c* bind and react with each other in different configurations resulting from the protein−protein interaction termed as the gating process for electron transfer (*36*−*38*), showing possible configurations for the diprotein complex by computer simulation (*29*, *39*).

We have previously shown that charged peptides may be useful for studies on the molecular recognition character of the protein and its interaction-induced structural change (*40*−*42*). Actually, positively charged lysine peptides interacted with the consecutive Asp and Glu residues of the negative patch of PC (Figure 1) and competitively inhibited electron transfer from reduced cyt *c* to oxidized PC (*40*). The inhibitory effects of oligolysine on electron transfer were explained as competitive inhibition due to neutralization of the PC negative patch by formation of PC·oligolysine complexes. Changes in the active site Cu−Cys geometry and a shift to a higher redox potential for PC on binding of oligolysine were also observed (*40*), suggesting that oligolysine induces a structural change in PC to make the copper site adapted for facile electron transfer.

Tyr83 which is located near the negative patch has been proposed to be involved in electron transfer from cyt *f* or cyt *c* to PC, since the reaction rate decreased upon replacement of Tyr with other amino acid residues (*31*, *32*). Ullmann et al. recently demonstrated by molecular dynamics a possibility of a cation−π interaction at the Tyr83 site, which might be important for electron transfer from cyt *f* to PC (*29*). On the other hand, Tyr83 mutants showed minor effects on the interaction between PC and PSI, and electron transfer from PC to $P700^+$ was suggested to occur at the hydrophobic patch (*43*−*45*). In this study, we investigated the interaction of Tyr83 mutants of PC with oligolysines with a view of obtaining detailed information on the structural change at the active site of PC associated with the interaction at the PC negative patch.

Table 1: Nucleotide Sequences of the Primers

primer	sequence[a]
PCY83Fa	ATACAAGTTTTTCTGTGCCCCTC
PCY83Fb	GAGGGGCACAGAAAAACTTGTAT
PCY83Sa	ATACAAGTTTTCCTGTGCCCCTC
PCY83Sb	GAGGGGCACAGGAAAACTTGTAT
PCY83La	ATACAAGTTTTTATGTGCCCCTC
PCY83Lb	GAGGGGCACATAAAAACTTGTA
PCY83Ha	ATACAAGTTTCACTGTGCCCCTC
PCY83Hb	GAGGGGCACAGTGAAACTTGTAT

[a] Underlines indicate the nucleotides for the modified amino acid.

EXPERIMENTAL PROCEDURES

Site-Directed Mutagenesis and Protein Purification. Enzymes for site-directed mutagenesis were obtained from New England Biolabs, Inc. (Berverly, MA), Boehringer GmbH (Mannheim, Germany), and Takara Shuzo Co. (Kyoto, Japan). Oligonucleotide primers were purchased from Katayama Kagaku Kogyo Co. (Osaka, Japan). Amino acid substitutions of PC at the Tyr83 position were introduced by PCR-based in vitro mutagenesis (*46*) of a PC-expression vector as follows: Using a pBluescript KS (Stratagene)-derived plasmid which carried the cDNA of the *Silene pratensis* (white campion) precursor PC (*47*, *48*) as a template, two DNA segments were initially amplified with T7 and PC-Y83Xa (Table 1) primers and M13-reverse and PC-Y83Xb (Table 1) primers, respectively, and then purified. The overlap region of the two PCR products was successively extended by an additional PCR with T7 and M13-reverse primers. The resulting PCR product, which contained the full-length cDNA of the mutant silene precursor PC, was digested with *Bam*HI and *Nco*I and inserted into the *Bam*HI−*Nco*I site of the pET3d expression vector (Novagen, Madison, WI). The obtained plasmids were introduced into *Escherichia coli* BL21(DE3) by electroporation with an electric pulse generator (Celljject Basic; EquiBio s.a., Angleur, Belgium). Plasmid DNAs were prepared by the boiling lysis or alkaline methods (*49*). DNA sequencing was carried out with a Taq DyeDeoxy terminator cycle sequencing kit (Applied Biosystems, Inc., Foster City, CA) and a model 310 DNA sequencing system (Applied Biosystems, Inc.). DNA sequences were analyzed with DNASIS software (version 3.6; Hitachi Software Engineering, Yokohama, Japan). Oxidized wild-type and Tyr83 mutant PCs (Y83F, Y83S, Y83L, and Y83H) were purified as described (*20*, *48*), and the purities of the proteins were confirmed by the ratio of the absorbance (Abs) at 280 nm to that at 597 nm ($Abs_{280}/Abs_{597} < 1.30$).

Oxidized PC was dissolved in 10 mM phosphate buffer, pH 7.4, with a certain amount of oligolysine. *Tetra*-Lys and

Table 2: Absorption Maximum Wavelengths, Average ν_{Cu-S} Frequencies, EPR Parameters, and Midpoint Redox Potentials ($E_{midpoint}$) of Wild-Type and Tyr83 Mutant PCs

species	wavelength[a] (nm)	ν_{Cu-S}[b] (cm^{-1})	EPR parameters $g_{\|\|}$	EPR parameters $\|A_{\|\|}\|$	$E_{midpoint}$[c] (mV)
wild-type	597.5	418.4	2.242	6.2	344
Y83F	597.5	417.9	2.256	5.7	340
Y83S	595.5	420.6	2.239	6.5	325
Y83L	595.5	423.3	2.238	6.5	320
Y83H	598.0	417.0	2.246	6.2	382

[a] Error ±0.5 nm. [b] Error ±1.0 cm^{-1} for the calculated values. [c] vs NHE; measured in 10 mM phosphate buffer, pH 7.4; error ±5 mV.

penta-Lys were purchased from Sigma, and 2−10 mM oligopeptide solutions were obtained by dissolving the peptides in the corresponding buffer and then adjusting the pH. The concentrations of PC were adjusted by its absorption maximum around 600 nm.

Spectroscopic Measurements. Absorption spectra of oxidized PC with and without oligolysines were measured at 15 °C on a Shimadzu UV-3100PC spectrophotometer. Circular dichroism (CD) spectra were obtained at 15 °C with a JASCO J-720 spectropolarimeter in a 2-cm path length quartz cell. Resonance Raman (RR) scattering was excited at 591 nm with an Ar^+ ion laser (Spectra Physics, 2017)-pumped dye laser (Spectra Physics, 376) with Rhodamine 6G, and detected with a triple polychromator (JASCO, NR-1800) equipped with a CCD detector (Princeton Instruments). The slit width and slit height were set to be 200 μm and 10 mm, respectively. The excitation laser beam power (at the sample point) was adjusted to 60 mW. RR measurements were carried out at ambient temperature with a spinning cell (3000 rpm). The data accumulation time was 400 s. Raman shifts were calibrated with CCl_4 and toluene, and the accuracy of the peak positions of the Raman bands was ±1 cm^{-1}. EPR spectra were measured at 77 K with a JES-RE1X EPR spectrophotometer (JEOL, Tokyo, Japan). The frequency, microwave power, and modulation for the EPR measurements were 9.230 GHz, 1 mW, and 0.63 mT, respectively. Cyclic voltammetry was carried out at ambient temperature with a voltammetric analyzer (Bioanalytical Systems, 100B). A 2-diethylaminoethanethiol (Sigma) modified gold electrode, prepared as described previously (*50*), was used as a working electrode, and a gold wire and an Ag/AgCl electrode were used as counter and reference electrodes, respectively (*40*, *50*, *51*). The midpoint redox potentials were calibrated by using the redox potential of $[Co(phen)_3]^{2+/3+}$ (*13*).

RESULTS AND DISCUSSION

Absorption Spectral Changes on Oligolysine Binding. Intense absorption bands around 600 nm which have been assigned to the cysteine thiolate [S(Cys)]-to-Cu(II) charge transfer (CT) band (*1*, *2*) were observed in the absorption spectra of oxidized wild-type and Tyr83 mutant PCs, and their absorption maximum wavelengths are listed in Table 2. Y83F mutant PC exhibited a maximum wavelength similar to that of wild-type PC, whereas the maximum wavelengths of Y83S and Y83L PCs were lower and the corresponding wavelength of Y83H PC was higher, respectively, than that of wild-type PC. The difference absorption spectra between Tyr83 mutant PCs and wild-type PC (Tyr83 mutant PC *minus* wild-type PC), shown in Figure 2A, clearly demonstrate these

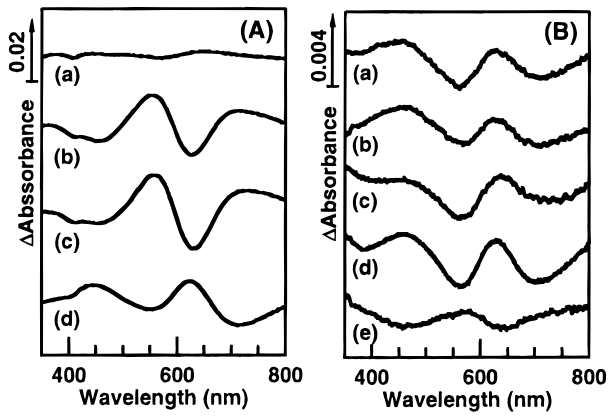

FIGURE 2: (A) Difference absorption spectra obtained by subtracting the spectrum of oxidized wild-type PC (100 μM) from the spectra of oxidized Tyr83 mutant PCs (100 μM): Y83F (a), Y83S (b), Y83L (c), and Y83H (d) proteins. (B) Difference absorption spectra of oxidized wild-type and Tyr83 mutant PCs (100 μM) obtained by subtracting their spectra from those with *tetra*-Lys (360 μM): wild-type (a), Y83F (b), Y83S (c), Y83L (d), and Y83H (e) proteins. Phosphate buffer (10 mM), pH 7.4, was used. All measurements were performed at 15 °C.

wavelength shifts. In the difference spectra of Y83S, Y83L, and Y83H proteins, peaks and troughs were detected at about 460, 560, 630, and 700 nm, while the intensities of these difference peaks decreased significantly for the Y83F protein. These peaks in the difference spectra revealed that species with a longer wavelength for the 600-nm absorption band exhibit increase and decrease in the intensities of the 460- and 700-nm absorption bands, respectively.

The difference absorption spectra of oxidized wild-type and Tyr83 mutant PCs in the presence and absence of *tetra*-Lys are shown in Figure 2B. A factor of 0.99−1.01 was used to make each difference pattern similar to that of wild-type PC between with and without *tetra*-Lys obtained using a tandem cell. Peaks (at about 460 and 630 nm) and troughs (at about 560 and 700 nm) were detected in the difference spectra of wild-type, Y83F, Y83S, and Y83L proteins, which demonstrate changes in their absorption spectra on interaction with *tetra*-Lys. The peaks and troughs in the difference spectra indicate a shift of the 600-nm band to a slightly longer wavelength and an increase in the intensity of the 460-nm band. Since the 600-nm band is assigned to the S(Cys)-to-Cu(II) LMCT band (*1*, *2*), the structure of the Cu site [at least the Cu−S(Cys) bond] should be altered by addition of *tetra*-Lys. These spectral changes were previously attributed to binding of oligolysine to the negative patch of PC by the use of the negative patch mutant PCs (*40*), and the structural change at the Cu site could be regarded as a result of the gating process as postulated by Kostić et al. (*36*−*38*, *52*). Considering that the changes were also observed in the absorption spectra of Tyr83 mutant PCs upon interaction with oligolysine at the negative patch, the force for the structural change may not be transmitted through the Tyr83 residue, while electron transfer from cyt *f* to the active site of PC is suggested to pass through the Tyr83 residue (*31*, *32*). The force for the structural change may transmit through the peptide backbone to His37 and thus the copper site, although there could be alternative mechanisms.

The pattern in the difference spectrum of the Y83H protein with and without *tetra*-Lys was different from the patterns

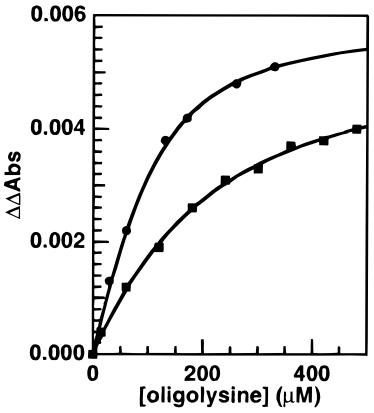

FIGURE 3: Plots of ΔΔAbs vs [oligolysine], together with least-squares fitted lines according to eq 2. ■ = *tetra*- and ● = *penta*-Lys. The concentration of PC was 100 μM.

of wild-type and other mutant PCs. The absorption maximum wavelength for the 600-nm band of the Y83H protein did not change on addition of 1 M NaCl to the protein solution (data not shown), which suggests that hydrogen bonding in the Y83H protein is not the major factor to cause the structural perturbation at the active site. In the absence of *tetra*-Lys, the 600-nm band of the Y83H protein exhibited its peak at a longer wavelength than that of wild-type PC (Figure 2). This shift was similar to that observed for wild-type PC on oligolysine binding. The active site structure of the Y83H protein may therefore be perturbed to a structure similar to that of wild-type PC bound with oligolysine, and the additional structural change of the Y83H protein on oligolysine binding might be different from the structural changes observed for other species.

The structural change due to oligolysine binding should be based on an equilibrium between oxidized PC and oligolysine, because the intensities of the peaks and troughs in the difference spectra increased with the concentration of oligolysine (*40*). The observed intensity changes in the absorption spectra may be interpreted by considering formation of a 1:1 PC·oligolysine complex by the equation:

$$\mathrm{PC} + \mathrm{oligolysine} \overset{K_i}{\rightleftharpoons} \mathrm{PC{\cdot}oligolysine} \qquad (1)$$

where K_i is the association constant for PC·oligolysine. If we write the difference between the observed absorption changes at 630 and 560 nm upon oligolysine binding as ΔΔAbs, the difference between the absorption coefficient changes at 630 and 560 nm upon oligolysine binding as $\Delta\Delta\epsilon$, the concentrations of PC and oligolysine as [PC] and [oligolysine], respectively, and the cell length used for the measurements as l, we obtain the relationship:

$$\Delta\Delta\mathrm{Abs} = \frac{\Delta\Delta\epsilon \times l}{2}\left\{\left([\mathrm{PC}] + [\mathrm{oligolysine}] + \frac{1}{K_i}\right) - \left[\left([\mathrm{PC}] + [\mathrm{oligolysine}] + \frac{1}{K_i}\right)^2 - 4\,[\mathrm{PC}][\mathrm{oligolysine}]\right]^{1/2}\right\} \qquad (2)$$

Plots of ΔΔAbs vs [oligolysine] are shown in Figure 3 with least-squares fitting with eq 2, which gave $\Delta\Delta\epsilon$ (=60 ± 10 $M^{-1}cm^{-1}$) and K_i (=8000 ± 4000 and 24 000 ± 7000 M^{-1} for *tetra*- and *penta*-Lys, respectively). Since the fitting

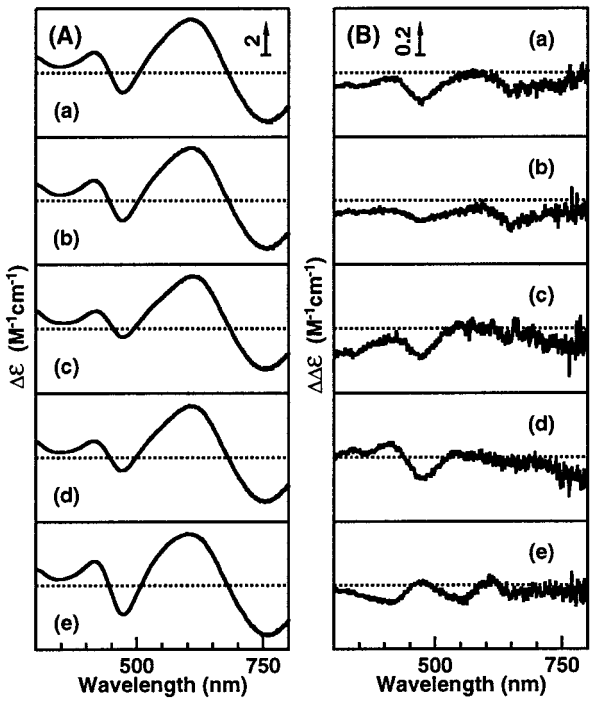

FIGURE 4: (A) CD spectra of oxidized wild-type and Tyr83 mutant PCs (70 μM): wild-type (a), Y83F (b), Y83S (c), Y83L (d), and Y83H (e) proteins. (B) Difference CD spectra of oxidized wild-type and Tyr83 mutant PCs (70 μM) obtained by subtracting their spectra from those with *tetra*-Lys (600 μM): wild-type (a), Y83F (b), Y83S (c), Y83L (d), and Y83H (e) proteins. The baselines of the difference spectra are shown as dotted lines. Phosphate buffer (10 mM), pH 7.4, was used. All measurements were performed at 15 °C.

was successful, it is reasonable to assume that only one oligolysine was bound to the negative patch of PC, which is in agreement with the previous conclusion derived from the inhibitory character of oligolysine on electron transfer from cyt *f* or cyt *c* to PC (*40*, *42*). The association constants between PC and oligolysine obtained in this study from the absorption difference spectra were larger than those previously obtained from the electron-transfer experiments (*40*), which should be caused by addition of NaCl to the solution for electron transfer to make the rate detectable.

CD Spectral Changes on Oligolysine Binding. Since the CD spectra are very sensitive to the protein structures, CD measurements were performed for oxidized wild-type and Tyr83 mutant PCs (Figure 4A). The CD spectra of wild-type and Tyr83 mutant PCs all exhibited positive bands at about 420, 560, and 610 nm and negative bands at about 470 and 760 nm. However, the intensities of the 420- and 470-nm bands for the Y83L and Y83S proteins decreased, whereas those of the corresponding bands for the Y83H protein increased, respectively, compared to those of wild-type and Y83F proteins. These 420- and 470-nm bands have been assigned to the Met → Cu $3d_{x^2-y^2}$ and His π_1 → Cu $3d_{x^2-y^2}$ CT transitions, respectively (*1*). In cucumber basic protein, the intensities of the 420- and 470-nm CD bands increase (*4*), the Cu−S(Cys) and Cu−S(Met) bond lengths are expanded and contracted by 0.1 and 0.2 Å, respectively (*53*), and the Cu−S(Cys) stretching frequency decreases (*54*) compared with PC. Therefore, the Cu−S(Cys) and Cu−S(Met) bond lengths should be longer and shorter, respectively, for the Y83H protein compared with wild-type and

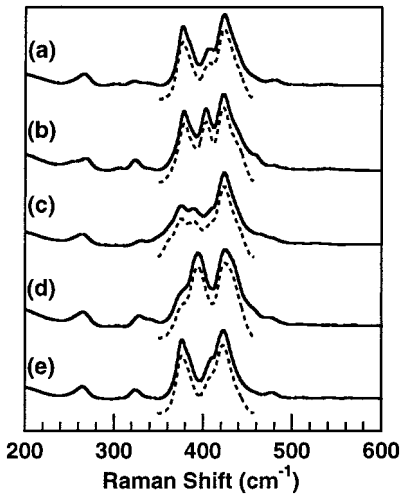

FIGURE 5: RR spectra in the 200−600-cm^{-1} region of oxidized wild-type and Tyr83 mutant PCs (500 μM): solid lines, observed spectra; broken lines, calculated spectra. Wild-type (a), Y83F (b), Y83S (c), Y83L (d), and Y83H (e) proteins. The ordinate scales in the spectra are normalized with the intensity of the 422-cm^{-1} band. Experimental conditions: excitation wavelength, 591.0 nm; laser power, 60 mW; slit width, 200 μm; slit height, 10 mm; buffer, phosphate buffer (10 mM), pH 7.4; measured at room temperature.

Y83F proteins, while the Y83L and Y83S proteins should have shorter Cu−S(Cys) and longer Cu−S(Met) bond lengths.

The difference CD spectra of oxidized wild-type and Tyr83 mutant PCs in the presence and absence of *tetra*-Lys are shown in Figure 4B. A positive peak at about 420 nm and a negative peak at about 470 nm were detected in the difference spectra of wild-type, Y83F, Y83S, and Y83L proteins, which demonstrate changes in their CD spectra and thus in the active site structure on interaction with *tetra*-Lys. These changes in the CD spectra on interaction with *tetra*-Lys were similar to the changes observed for the CD spectrum of the Y83H protein compared with that of the wild-type protein (Figure 4A, curves a and e), whose character was similar to that observed in the absorption spectra (Figure 2). Observation of CD spectral changes on interaction with *tetra*-Lys for several Tyr83 mutant PCs supports that the force for the structural change at the active site may not be transmitted through the Tyr83 residue. However, the difference CD spectrum of the Y83H protein showed opposite changes on interaction with *tetra*-Lys compared with other proteins, whose character was similar to that observed in the absorption spectra, probably due to perturbation of the structure of the Y83H protein similar to that of wild-type PC bound with oligolysine.

RR Spectra of Wild-Type and Tyr83 Mutant PCs with and without Oligolysine. RR spectroscopy is a powerful method for investigating the character of the Cu−S(Cys) bond in type 1 copper proteins by exciting the Raman scattering near the S(Cys)-to-Cu(II) CT band (*10*, *55*−*58*). Several bands were observed at 374−475 cm^{-1} for the RR spectra in the 200−600 cm^{-1} region of wild-type and Tyr83 mutant PCs excited at 591.0 nm (Figure 5), which is mainly due to the mixing of the Cu−S stretch with some angle bending of the coordinated Cys side chain (*10*, *55*−*58*). The weighted average frequency based on the S-isotope dependence has been shown to correlate with the Cu−S(Cys) distance for azurin, which is another type 1 copper protein, and its mutants (*9*). However, electronic coupling along both the remote and the adjacent electron-transfer pathways of PC has been suggested by identification of resonance-enhanced internal modes of the Cys84 and His87 ligands (*59*).

The RR spectra of oxidized PC have been discussed by deconvoluting them with bands at about 375, 385, 395, 405, 422, 430, and 440 cm^{-1} (*57*, *59*). Likewise, the obtained Raman spectra of wild-type and Tyr83 mutant PCs in Figure 5 were fitted with Gaussian bands at about 365, 375, 385, 395, 405, 422, 430, and 440 cm^{-1} (bandwidths of 12, 13, and 14 cm^{-1} for the 365-, 375-, and 385−440-cm^{-1} bands, respectively). The sum of the calculated bands is also depicted in Figure 5, and the obtained frequencies with their relative intensities are listed in Table 3. Since mainly the 375-, 422-, and 430-cm^{-1} bands contain major contribution from ν_{Cu-S} (*59*), the average ν_{Cu-S} frequencies of wild-type and Tyr83 mutant PCs were calculated from the intensities and frequencies of these three fitted bands based on the reported $\Delta^{32}S/^{34}S$ isotope shifts (*59*) and are listed in Table 2. The average ν_{Cu-S} frequency obtained in this study was in the order Y83L > Y83S > Y83F ≈ wild-type > Y83H, suggesting a stronger Cu−S(Cys) bond in this order. The species with a shorter wavelength for the S(Cys)-to-Cu(II) CT band exhibited a higher average ν_{Cu-S} frequency and thus a stronger Cu−S(Cys) bond.

Figure 6 shows the difference RR spectra with and without *tetra*-Lys for oxidized wild-type and Tyr83 mutant PCs, where peaks and troughs were detected in all the difference spectra. We previously reported similar peaks and troughs for wild-type PC on oligolysine binding and attributed them to the perturbation of the Cu−S(Cys) geometry on oligolysine binding (*40*). However, the 267-cm^{-1} band, which is assigned to the Cu−His stretching mode (*60*), did not show any change for either wild-type or any Tyr83 mutant PC on addition of oligolysine to their solutions. When *tetra*-Lys was added to the wild-type and Tyr83 mutant PC solutions, the bands at 375−475 cm^{-1} slightly shifted to lower frequencies and the intensities of some lower frequency bands in this region increased slightly. Especially, the ν_{Cu-S}-related 375- and 422-cm^{-1} bands were affected. These results indicate that the Cu−S(Cys) bond was weakened a little on addition of oligolysine. However, Y83F and Y83H proteins showed smaller peaks in the difference RR spectra compared to those of the other species, which was similar to that observed in the difference absorption and CD spectra (Figures 2B and 4B).

EPR Measurements. The EPR spectra of oxidized wild-type and Tyr83 mutant PCs are shown in Figure 7, and their EPR parameters are listed in Table 2. The correlation between the rhombicity of the EPR spectrum and the increase of the 460-nm absorption band has been mentioned for type 1 copper proteins (*5*). The rhombic distortion in these proteins has been suggested to be due to the strengthening of the Cu−axial ligand bond (*6*). The stronger Cu−S(Met) axial bond was proposed to cause a larger displacement of the Cu(II) from the trigonal plane with two histidine nitrogen atoms and one cysteine sulfur atom, shifting the active site coordination structure toward a tetrahedral geometry (*5*). The Y83S and Y83L proteins both showed smaller $g_{\|}$ and larger $|A_{\|}|$ values, a more axial EPR spectrum, compared to those of

Table 3: Calculated Raman Frequencies and Their Relative Intensities for the RR Spectra of Wild-Type and Tyr83 Mutant PCs

species	frequency[a] (cm^{-1})							
wild-type	364.8 (0.08)	375.4 (0.59)	385.2 (0.38)	394.6 (0.13)	405.6 (0.55)	421.6 (1.0)	434.0 (0.51)	441.8 (0.27)
Y83F	366.7 (0.18)	377.5 (0.55)	387.7 (0.37)	–	403.0 (0.88)	421.3 (1.0)	432.0 (0.46)	442.1 (0.36)
Y83S	362.8 (0.29)	374.5 (0.38)	384.4 (0.28)	393.3 (0.44)	407.7 (0.49)	422.0 (1.0)	433.0 (0.50)	442.0 (0.33)
Y83L	367.9 (0.15)	376.0 (0.29)	386.3 (0.37)	394.4 (0.94)	406.3 (0.44)	421.7 (1.0)	432.8 (0.78)	443.1 (0.33)
Y83H	365.0 (0.10)	375.3 (0.61)	384.9 (0.43)	396.8 (0.18)	408.2 (0.53)	421.5 (1.0)	431.6 (0.46)	442.3 (0.21)

[a] Error of the frequency differences between the fitted bands is ± 0.2 cm^{-1}. Relative intensities with the 422-cm^{-1} band are listed in parentheses.

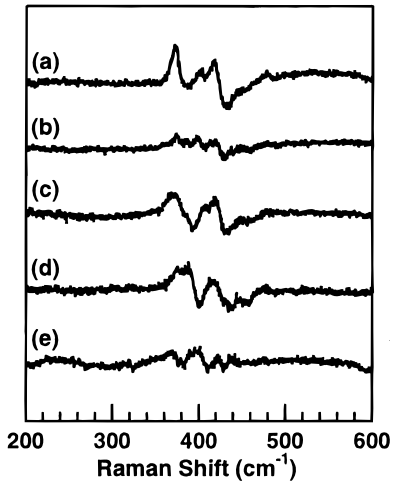

FIGURE 6: Difference RR spectra in the 200−600-cm^{-1} region of oxidized wild-type and Tyr83 mutant PCs (500 μM) obtained by subtracting their spectra from those with *tetra*-Lys (900 μM): wild-type (a), Y83F (b), Y83S (c), Y83L (d), and Y83H (e) proteins. The ordinate scales in the spectra are normalized with the intensity of the 422-cm^{-1} band. Experimental conditions were the same as those in Figure 5.

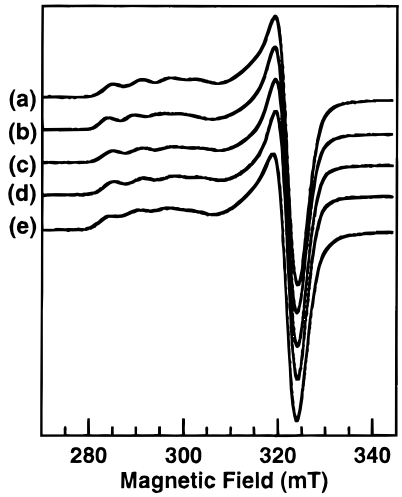

FIGURE 7: EPR spectra of oxidized wild-type and Tyr83 mutant PCs (600 μM): wild-type (a), Y83F (b), Y83S (c), Y83L (d), and Y83H (e) proteins. Experimental conditions: microwave power, 1 mW; frequency, 9.230 GHz; modulation, 0.63 mT; measured at 77 K.

the wild-type protein, suggesting a more trigonal geometry for Cu(II). However, no significant change was detected in the EPR parameters of PC on addition of *tetra*- or *penta*-Lys to the protein solution. This might be due to the small change of the EPR signals compared to the absorption and RR spectra.

Electrochemical Measurements. Cyclic voltammograms obtained for wild-type and Tyr83 mutant PCs showed well-defined quasi-reversible faradaic responses with the midpoint redox potentials listed in Table 2. Y83F mutant PC exhibited a redox potential similar to that of wild-type PC, whereas the redox potentials of Y83S and Y83L PCs shifted to lower potentials and the redox potential of Y83H PC shifted to a higher potential, respectively, compared with that of wild-type PC. It is noteworthy that species with a longer maximum wavelength for the 600-nm absorption band and a lower average ν_{Cu-S} frequency exhibited a higher redox potential. Likewise, the redox potential of wild-type PC shifted to a higher potential upon oligolysine binding, which was associated with spectroscopic changes of a longer maximum wavelength for the 600-nm absorption band and a lower average ν_{Cu-S} frequency (*40*).

Correlation among Spectroscopic and Electrochemical Properties of PC. Comparison between several type 1 copper proteins has shown that proteins with a higher energy ligand field associated with rotation of the Cu $d_{x^2-y^2}$ half-filled HOMO exhibit longer Cu−S(Cys) and shorter Cu−S(Met) bonds with a more tetrahedral geometry (*4*, *5*). The intensity increase of the 460-nm absorption band in type 1 copper proteins has been explained by the structural change from a trigonal planar toward a more tetrahedral Cu site geometry associated with the lengthening of the Cu−S(Cys) bond (*5*−*7*), and species exhibiting a more intense 460-nm absorption band has been shown to have a smaller average ν_{Cu-S} frequency in type 1 and type 2 copper cysteinate proteins obtained by site-directed mutagenesis (*10*). The spectroscopic and electrochemical properties of the wild-type and Tyr83 mutant PCs were similar but slightly different; e.g., species exhibiting a more intense 460-nm absorption band and a longer wavelength for the 600-nm absorption band in this study showed a more tetrahedral geometry for the Cu site and a smaller average ν_{Cu-S} frequency (Table 2). A weaker Cu−S(Cys) bond would create a weaker ligand field with the Cys ligand, and thus the energy of the S(Cys)-to-Cu(II) CT band would decrease. A weaker Cu−S(Cys) bond would also induce a structural change associated with a more tetrahedral geometry for the Cu(II) site and raise the redox potential of Cu, characteristics which have been observed by comparison of the Y83H protein with the Y83S and Y83L proteins (Table 2). Likewise, when wild-type PC interacted with oligolysine, the intensity of the 460-nm absorption band increased, the maximum wavelength for the 600-nm absorp-

tion band became longer, the average ν_{Cu-S} frequency became lower, and the redox potential shifted to a higher potential. All these changes would be associated with a slightly more tetrahedral geometry for the Cu site, further suggesting that PC suffers a structural change on interaction with its redox partner, cyt *f*, for facile electron transfer from it. Although the changes observed for PC on interaction with oligolysine were small, they may play an important role in controlling its function.

CONCLUSIONS

When wild-type PC interacted with oligolysine, the intensity of the 460-nm absorption band increased, the maximum wavelength for the 600-nm absorption band became longer, the intensities of the 420- and 470-nm CD bands increased, the average ν_{Cu-S} frequency became lower, and the redox potential shifted to a higher potential. These results demonstrate that the Cu−S(Cys) bond of the active site of PC is weakened when it interacts with oligolysine and thus could facilitate electron transfer from its redox partner, cyt *f*.

Since changes were observed for both wild-type and Tyr83 mutant PCs in their absorption, CD, and RR spectra on oligolysine binding, the structural change due to binding of oligolysine to PC should not be transmitted through the path of Tyr83−Cys84−copper site by a cation−π interaction which is proposed for electron transfer.

REFERENCES

1. Gewirth, A. A., and Solomon, E. I. (1988) *J. Am. Chem. Soc. 110*, 3811−3819.
2. Solomon, E. I., Baldwin, M. J., and Lowery, M. D. (1992) *Chem. Rev. 92*, 521−542.
3. Pierloot, K., De Kerpel, J. O. A., Ryde, U., Olsson, M. H. M., and Roos, B. O. (1998) *J. Am. Chem. Soc. 120*, 13156−13166.
4. LaCroix, L. B., Randall, D. W., Nersissian, A. M., Hoitink, C. W. G., Canters, G. W., Valentine, J. S., and Solomon, E. I. (1998) *J. Am. Chem. Soc. 120*, 9621−9631.
5. Lu, Y., LaCroix, L. B., Lowery, M. D., Solomon, E. I., Bender, C. J., Peisach, J., Roe, J. A., Gralla, E. B., and Valentine, J. S. (1993) *J. Am. Chem. Soc. 115*, 5907−5918.
6. Gewirth, A. A., Cohen, S. L., Schugar, H. J., and Solomon, E. I. (1987) *Inorg. Chem. 26*, 1133−1146.
7. Han, J., Loehr, T. M., Lu, Y., Valentine, J. S., Averill, B. A., and Sanders-Loehr, J. (1993) *J. Am. Chem. Soc. 115*, 4256−4263.
8. Blair, D. F., Campbell, G. W., Schoonover, J. R., Chan, S. I., Gray, H. B., Malmstrom, B. G., Pecht, I., Swanson, B. I., Woodruff, W. H., Cho, W. K., English, A. M., Fry, H. A., Lum, V., and Norton, K. A. (1985) *J. Am. Chem. Soc. 107*, 5755−5766.
9. Dave, B. C., Germanas, J. P., and Czernuszewicz, R. S. (1993) *J. Am. Chem. Soc. 115*, 12175−12176.
10. Andrew, C. R., Yeom, H., Valentine, J. S., Karlsson, B. G., Bonander, N., van Pouderoyen, G., Canters, G. W., Loehr, T. M., and Sanders-Loehr, J. (1994) *J. Am. Chem. Soc. 116*, 11489−11498.
11. Andrew, C. R., and Sanders-Loehr, J. (1996) *Acc. Chem. Res. 29*, 365−372.
12. Andrew, C. R., Han, J., den Blaauwen, T., van Pouderoyen, G., Vijgenboom, E., Canters, G. W., Loehr, T. M., and Sanders-Loehr, J. (1997) *J. Biol. Inorg. Chem. 2*, 98−107.
13. Sykes, A. G. (1991) *Struct. Bonding (Berlin) 75*, 175−224.
14. Redinbo, M. R., Yeates, T. O., and Merchant, S. (1994) *J. Bioenerg. Biomembr. 26*, 49−66.
15. Gross, E. L. (1993) *Photosynth. Res. 37*, 103−116.
16. Colman, P. M., Freeman, H. C., Guss, J. M., Murata, M., Norris, V. A., Ramshaw, J. A. M., and Venkatappa, M. P. (1978) *Nature 272*, 319−324.
17. Guss, J. M., and Freeman, H. C. (1983) *J. Mol. Biol. 169*, 521−563.
18. Guss, J. M., Harrowell, P. R., Murata, M., Norris, V. A., and Freeman, H. C. (1986) *J. Mol. Biol. 192*, 361−387.
19. Freeman, H. C. (1981) in *Coordination Chemistry−21* (Laurent, J. L., Ed.) pp 29−51, Pergamon Press, Oxford.
20. Lee, B. H., Hibino, T., Takabe, T., Weisbeek, P. J., and Takabe, T. (1995) *J. Biochem. 117*, 1209−1217.
21. Chapman, S. K., Knox, C. V., and Sykes, A. G. (1984) *J. Chem. Soc., Dalton Trans.*, 2775−2780.
22. Anderson, G. P., Sanderson, D. G., Lee, C. H., Durell, S., Anderson, L. B., and Gross, E. L. (1987) *Biochim. Biophys. Acta 894*, 386-398.
23. Adam, Z., and Malkin, R. (1989) *Biochim. Biophys. Acta 975*, 158−163.
24. Gross, E. L., and Curtiss, A. (1991) *Biochim. Biophys. Acta 1056*, 166−172.
25. Morand, L. Z., Frame, M. K., Colvert, K. K., Johnson, D. A., Krogmann, D. W., and Davis, D. J. (1989) *Biochemistry 28*, 8039−8047.
26. Qin, L., and Kostić, N. M. (1992) *Biochemistry 31*, 5145−5150.
27. Meyer, T. E., Zhao, Z. G., Cusanovich, M. A., and Tollin, G. (1993) *Biochemistry 32*, 4552−4559.
28. Roberts, V. A., Freeman, H. C., Olson, A. J., Tainer, J. A., and Getzoff, E. D. (1991) *J. Biol. Chem. 266*, 13431−13441.
29. Ullmann, G. M., Knapp, E.-W., and Kostić, N. M. (1997) *J. Am. Chem. Soc. 119*, 42−52.
30. He, S., Modi, S., Bendall, D. S., and Gray, J. C. (1991) *EMBO J. 10*, 4011−4016.
31. Modi, S., Nordling, M., Lundberg, L. G., Hansson, Ö., and Bendall, D. S. (1992) *Biochim. Biophys. Acta 1102*, 85−90.
32. Modi, S., He, S., Gray, J. C., and Bendall, D. S. (1992) *Biochim. Biophys. Acta 1101*, 64−68.
33. Ubbink, M., and Bendall, D. S. (1997) *Biochemistry 36*, 6326−6335.
34. Pearson, D. C., Jr., Gross, E. L. G., and David, E. S. (1996) *Biophys. J. 71*, 64−76.
35. Ubbink, M., Ejdebäck, M., Karsson, B. G., and Bendall, D. S. (1998) *Structure 6*, 323−335.
36. Crnogorac, M. M., Shen, C., Young, S., Hansson, Ö., and Kostić, N. M. (1996) *Biochemistry 35*, 16465−16474.
37. Ivković-Jensen, M. M., and Kostić, N. M. (1996) *Biochemistry 35*, 15095−15106.
38. Ivković-Jensen, M. M., and Kostić, N. M. (1997) *Biochemistry 36*, 8135−8144.
39. Ullmann, G. M., and Kostić, N. M. (1995) *J. Am. Chem. Soc. 117*, 4766−4774.
40. Hirota, S., Hayamizu, K., Endo, M., Hibino, T., Takabe, T., Kohzuma, T., and Yamauchi, O. (1998) *J. Am. Chem. Soc. 120*, 8177−8183.
41. Hirota, S., Endo, M., Tsukazaki, T., Takabe, T., and Yamauchi, O. (1998) *J. Biol. Inorg. Chem. 3*, 563−569.
42. Hirota, S., Endo, M., Hayamizu, K., Tsukazaki, T., Takabe, T., Kohzuma, T., and Yamauchi, O. (1999) *J. Am. Chem. Soc. 121*, 849−855.
43. Nordling, M., Sigfridsson, K., Young, S., Lundberg, L. G., and Hansson, Ö. (1991) *FEBS Lett. 291*, 327−330.
44. Sigfridsson, K., Young, S., and Hansson, Ö. (1996) *Biochemistry 35*, 1249−1257.
45. Haehnel, W., Jansen, T., Gause, K., Klösgen, R. B., Stahl, B., Michl, D., Huvermann, B., Karas, M., and Herrmann, R. G. (1994) *EMBO J. 13*, 1028−1038.
46. Horton, R. M. (1993) in *Methods in Molecular Biology* (White, B. A., Ed.) pp 251−261, Humana Press Inc., Totowa, NJ.
47. Hibino, T., de Boer, A. D., Weisbeek, P. J., and Takabe, T. (1991) *Biochim. Biophys. Acta 1058*, 107−112.

48. Hibino, T., Lee, B. H., and Takabe, T. (1994) *J. Biochem. 116*, 826−832.
49. Sambrook, J., Fritsch, E. F., and Maniatis, T. (1989) *Molecular Cloning; a Laboratory Manual*, 2nd ed., Cold Spring Harbor Laboratory Press, Cold Spring Harbor, NY.
50. Quinkal, I., Kyritsis, P., Kohzuma, T., Im, S.-C., Sykes, A. G., and Moulis, J.-M. (1996) *Biochim. Biophys. Acta 1295*, 201−208.
51. Kohzuma, T., Dennison, C., McFarlane, W., Nakashima, S., Kitagawa, T., Inoue, T., Kai, Y., Nishio, N., Shidara, S., Suzuki, S., and Sykes, A. G. (1995) *J. Biol. Chem. 270*, 25733−25738.
52. Qin, L., and Kostić, N. M. (1993) *Biochemistry 32*, 6073−6080.
53. Guss, J. M., Merritt, E. A., Phizackerley, R. P., and Freeman, H. C. (1996) *J. Mol. Biol. 262*, 686−705.
54. Sakurai, T., Sawada, S., and Nakahara, A. (1986) *Inorg. Chim. Acta 123*, L21−L22.
55. Sanders-Loehr, J. (1993) in *Bioinorganic Chemistry of Copper* (Karlin, K. D., and Tyeklár, Z., Eds.) pp 51−63, Chapman & Hall, New York.
56. Woodruff, W. H., Dyer, R. B., and Schoonover, J. R. (1988) in *Biological Applications of Raman Spectroscopy* (Spiro, T. G., Ed.) pp 413−438, John Wiley, New York.
57. Qiu, D., Dong, S., Ybe, J. A., Hecht, M. H., and Spiro, T. G. (1995) *J. Am. Chem. Soc. 117*, 6443−6446.
58. Qiu, D., Dasgupta, S., Kozlowski, P. M., Goddard, W. A., III, and Spiro, T. G. (1998) *J. Am. Chem. Soc. 120*, 12791−12797.
59. Dong, S., and Spiro, T. G. (1998) *J. Am. Chem. Soc. 120*, 10434−10440.
60. Nestor, L., Larrabee, J. A., Woolery, G., Reinhammar, B., and Spiro, T. G. (1984) *Biochemistry 23*, 1084−1093.

BI9929812